Int. J. Therm. Sci. (1999) 38, 315–323

Ignition of epoxy by a high radiation source. A numerical study

Javad A. Esfahani*, Antonio C.M. Sousa**

Department of Mechanical Engineering, University of New Brunswick P.O.Box 4400, Fredericton, N.B., Canada E3B 5A3

(Received 2 June 1998, accepted 15 October 1998)

Abstract — The transient, two dimensional non-charring materials version of a numerical model developed to study the ignition of charring and non-charring materials is used to analyse the ignition process of epoxy when subjected to a monochromatic radiation source. The model has the significant feature of coupling the solution for the solid and gas phases through the boundary conditions at the gas/solid interface along with a global finite-rate thermal degradation for the solid phase. The predictions yield physically realistic results, and predicted ignition delays present a maximum deviation of 7.56 % when compared with published experimental data for an external radiation source with fluxes ranging from 1 $MW \cdot m^{-2}$ to 4 $MW \cdot m^{-2}$. © Elsevier, Paris.

epoxy / ignition delay / thermal degradation / radiation / numerical prediction / CFD

Résumé — Ignition de l'époxy par une source radiative de haute intensité. Une étude numérique. On a analysé le processus d'ignition de l'époxy lorsque celui-ci est soumis à une source radiative monochromatique. Pour ce faire, on a utilisé un modèle numérique transitoire et bidimensionnel applicable à des matériaux sans résidu. Ce modèle constitue une version d'un modèle plus général conçu pour des matériaux avec et sans résidu. Le modèle possède la caractéristique particulière de pouvoir coupler les solutions pour les phases solide et gazeuse par l'intermédiaire des conditions frontières à l'interface gaz–solide. Il permet, de plus, de tenir compte de la cinétique globale de la dégradation thermique de la phase solide. Les prédictions obtenues sont réalistes : les délais d'ignition calculés présentent une différence maximale de 7,56 %, si on les compare aux données expérimentales de la littérature pour le cas d'une source radiative externe produisant des flux entre 1 et 4 $MW \cdot m^{-2}$. © Elsevier, Paris.

époxy / délai d'ignition / dégradation thermique / rayonnement / prédiction numérique / CFD

Nomenclature

A	pre-exponential factor of reaction	$m \cdot s^{-1}$
c	specific heat	$J \cdot kg^{-1} \cdot K^{-1}$
E	activation energy	$J \cdot mol^{-1}$
g	gravitational acceleration	$m \cdot s^{-2}$
I	intensity of the radiative heat flux	$W \cdot m^{-2}$
k	thermal conductivity	$W \cdot m^{-1} \cdot K^{-1}$
M	molecular weight	$g \cdot mol^{-1}$
m	mass rate of volatiles	$g \cdot s^{-1}$
P	pressure	$N \cdot m^{-2}$
Pr	Prandtl number	
R	universal gas constant	$J \cdot K^{-1} \cdot mol^{-1}$
r	rate of pyrolysis reaction	s^{-1}
S	generic source term	$kg \cdot m^{-2} \cdot s^{-2}$ (momentum); $kg \cdot m^{-3} \cdot s^{-1} \cdot K$ (energy); $kg \cdot m^{-3} \cdot s^{-1}$ (mass fraction)
Sc	Schmidt number	
T	temperature	K
t	time	s
U	x component velocity	$m \cdot s^{-1}$
$\vec{U}$	vector of velocity	$m \cdot s^{-1}$
V	y component velocity	$m \cdot s^{-1}$
x	co-ordinate	m
Y	mass fraction	
y	co-ordinate	m

Greek symbols

β	volumetric thermal expansion coefficient	K^{-1}
Γ	generic diffusion coefficient	$kg \cdot m^{-1} \cdot s^{-1}$

* Present address: Department of Mechanical Engineering, Faculty of Engineering, Ferdowsi University of Mashhad, P.O.Box 91775-1111, Mashhad, Iran.
esfahani@unb.ca

** Correspondence and reprints.
asousa@unb.ca

ΔH	heat of combustion	$J \cdot kg^{-1}$
Δh	heat of degradation	$J \cdot kg^{-1}$
μ	absolute viscosity	$kg \cdot m^{-1} \cdot s^{-1}$
ν	stoichiometric ratio	
ρ	density	$kg \cdot m^{-3}$
κ	radiation absorption coefficient	$N^{-1} \cdot m$

Subscripts

F	fuel
g	gas
i	chemical species
ig	ignition
O	oxygen
s	solid
v	volatiles
0	initial conditions

1. INTRODUCTION

The versatility of epoxy resins makes them suitable for use as base materials, adhesives, or sealants in a wide range of industrial applications including aircraft structures, building and highway construction, maintenance and finishing products, and electronic boards. Their extensive use renews concern regarding issues of fire safety and prevention, and recent analyses of several aircraft accidents have identified the implication and contribution of these materials in and to fire propagation and flash-over [1].

Fire initiation of solid materials has been the focus of numerous experimental and theoretical investigations. However, despite the large volume of work already performed, the physically complex intervening mechanisms remain to be fully understood. In this area a major challenge is the formulation of a theoretical model capable of describing the ignition of actual solid materials. This model would provide not only the background for a better understanding of combustion phenomena, but also the basis for materials fire safety and enhanced design of fire detection and protection devices.

Analytical and numerical models have been reported possessing different degrees of sophistication. However, the complexity of the ignition process requires different assumptions to make the problem tractable. For instance, the ignition delay often is predicted without solving the equations for the surrounding air flow, which is the case of the analytical work of Ohlemiller and Summerfield [2], and of the numerical work of Nelson et al. [3]. The momentum and species equations were included, for example, in the one-dimensional model with attenuation of radiation in the solid and gas phases proposed by Di Blasi et al. [4], and in the model of Chandrasekaran et al. [5] where the attenuation of radiation in the solid and gas phases is not considered.

The primary mode of energy transfer in fire initiation and propagation is thermal radiation, as has been well-established in existing studies, among others, by Quintiere [6] for room fires and by Ramachandra [7] for microgravity fires. The energy transfer is affected by the radiation attenuation caused by the solid material itself and/or by the volatiles resulting from the solid decomposition, in particular those with strong absorption bands. The radiation properties, in particular surface reflectance and absorption, and gas absorption, vary greatly with the source wavelength, which adds a further degree of difficulty to the analysis and understanding of the ignition process. To circumvent this particular difficulty in the present work, the process will be studied for a monochromatic radiation source. Relevant information and experimental guidance for this study are found in Kashiwagi [8] for the radiation absorption by the concentration plume formed by the gaseous decomposition products, and in Ohlemiller and Summerfield [2] who indicate that in-depth radiation absorption can have a very strong effect on ignition data obtained with a radiative energy source.

2. MATHEMATICAL MODEL

In the present work, the transient, two-dimensional, non-charring materials version of a numerical model developed to study the ignition process [9] is used to emulate the experiments reported in Ohlemiller and Summerfield [2]. In these experiments, solid samples were irradiated by a continuous CO_2 laser beam (10.6 μm) in a quiescent atmosphere oxygen chamber for auto ignition tests. The primary objective was to study the influence of the external radiant heat flux upon the ignition delay.

2.1. Assumptions

In view of the complexity of the physical situation, and to simplify the modelling approach the following assumptions were made:

i) negligible surface regression;

ii) constant thermal properties;

iii) negligible radiation from the reacting volatiles to the solid surface;

iv) no photo-degradation;

v) negligible storage of mass and energy in the interior of the solid due to the volatiles;

vi) migration of volatiles within the solid is only towards the interface surface;

vii) the air within the solid is at constant pressure;

viii) the circular beam is approximated by a square cross-section beam.

The first two assumptions, i) and ii), require some caution, as their validity is not universal and may

not apply in cases dealing with high temperature and/or high temperature gradients, but in general they are reasonable for ignition threshold and early fire development. Assumption iii) is acceptable for fires occurring in pans with a characteristic length less than 0.1 m [10], which corresponds to the cases to be analysed in this study. Assumption iv) is satisfied because the radiation from an external source, as used in the laboratory tests, has the visible or infrared wavelength with a lower quantum energy than the bond dissociation energy of molecules [11]. For example, the quantum energy of a CO_2 laser beam estimated with Planck's law is 11 kJ·mol^{-1}, which is an order of magnitude less than the dissociation energy of chemical bonds. Assumptions v) and vi) are valid when the characteristic time of the intraparticle fluid flow, based on the characteristic diameter of the pores or tracheids through which volatiles escape, is shorter than the characteristic time of the solid degradation. Assumption viii) is valid when the heat diffusion scale in the radial direction is much smaller than that in the vertical direction, i.e.,

$$k/R^2 << k/L^2 \tag{1}$$

where k, R, and L are thermal conductivity, radius of the beam, and diffusion length in the vertical direction, respectively. The diffusion length in the vertical direction can be scaled by $(\alpha t)^{1/2}$, and replacing this in equation (1) results in:

$$k/R^2 << k/\alpha t \tag{2}$$

or

$$t << R^2/\alpha \tag{3}$$

this condition is satisfied for all cases studied for the ignition process.

2.2. Formulation

A schematic diagram of the physical configuration to be analysed along with the co-ordinate system and boundary conditions is shown in *figure 1*. The solid region is located at the lower end of the computational domain, while the air–combustion gases buoyancy-driven flow occurs above the solid. The ignition is initiated by incident radiation that heats up the solid upper surface.

The mathematical model follows closely that reported in Esfahani [12] and Esfahani [9], and it is largely based on the model proposed by Ohlemiller [13]. The unique feature of the present model is the coupling of the solution for the solid and gas phases through the boundary conditions at the gas – solid interface. The model also includes a global finite – rate thermal degradation for the solid phase and a global finite – rate combustion kinetics for the gas phase, as well as

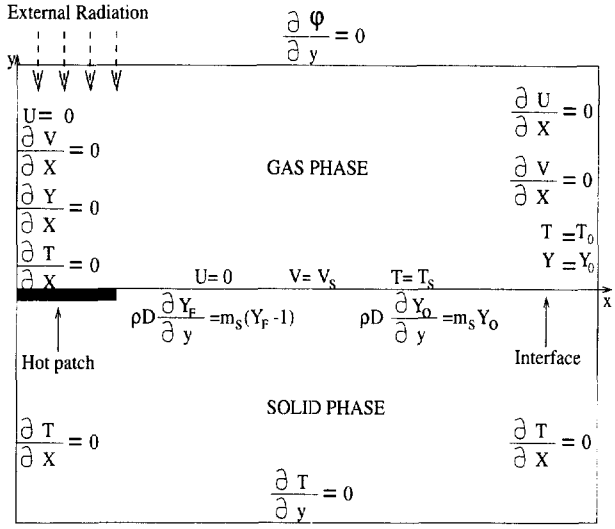

Figure 1. Physical configuration of radiative ignition of a solid fuel in quiescent air, including the boundary conditions used in the simulation.

in-depth absorption of radiation in the solid, and the attenuation of radiation by the gas phase. Both radiation effects are assumed to be governed by Beer's law [14].

The main components of the model are succinctly summarized in *table I*. The model incorporates the partial differential equations governing continuity, momentum, and energy for the gaseous phase, and mass fraction for oxygen and volatiles, respectively. For the solid phase, the constitutive relations describe kinetics of pyrolysis, consumption of the solid phase, mass balance of volatiles, and energy balance.

3. COMPUTER MODEL

The non-linear coupled partial differential equations are integrated by the control volume formulation to obtain the discretized equation set [15]. The convective/diffusive link coefficients are based on the hybrid scheme. The present formulation also uses a staggered grid where the velocity vectors are computed at the centre of each control volume face with the scalar values computed at the centre of the control volume. The equations governing fluid flow, continuity and momentum equations, are solved using the SIMPLEC procedure developed by Van Doormal and Raithby [16] which is an enhancement to the basic SIMPLE algorithm [15] and tends to provide improved solution times and numerical stability. The discrete equation sets are solved iteratively using a TDMA algorithm in conjunction with an additive correction multigrid strategy [17], as proposed by Lopes et al. [18] in their study of wildland fires.

TABLE I
Mathematical model.

Gas phase model

$$\frac{\partial(\rho\phi)}{\partial t} + \nabla\cdot\left(\rho\vec{U}\phi\right) = \nabla\cdot(\Gamma\nabla\phi) + S_\phi \qquad \phi = 1, u, v, T, Y_i, h$$

Equation	ϕ	Γ_ϕ	S_ϕ
Continuity	1	0	0
Momentum:			
x-direction	u	μ	$-\frac{\partial P}{\partial x}$
y-direction	v	μ	$-\frac{\partial P}{\partial y} + \rho g \beta (T - T_0)$
Mass fraction:			
fuel (F)	Y_F	$\frac{\mu}{Sc}$	$-A_g \exp(-E_g/RT)\, Y_O\, Y_F \rho^2 \; (= S_F)$
oxygen (O)	Y_O	$\frac{\mu}{Sc}$	$S_F\, \nu_O\, M_O/M_F$
Energy	T	$\frac{\mu}{Pr}$	$\frac{-S_F \triangle H - \kappa P_F I_0 \exp(-\kappa P_F y)}{c_g}$

Solid phase model

Kinetics of pyrolysis: $r = A\, exp(-E/RT_s)$

Consumption of solid: $\partial\rho_s/\partial t = -r\,\rho_s$

Mass balance of volatiles: $\partial m/\partial y = r\,\rho_s$

$$m = \int_0^y r\,\rho_s\,dy$$

Energy balance: $\rho_s\, c_s\, \partial T_s/\partial t + (T_s - T_0)\,\rho_s\,(-c_s\, r + c_v\, r) + m\, c_v\, \partial T_s/\partial y = \nabla\cdot(k_s\,\nabla T_s) + r\triangle h - \kappa_s\, I_0 \exp(-\kappa_s\, y)$

Based on tests conducted with the model for different time steps and grid sizes, it was found that slow convergence and even numerical instability may arise at the threshold of ignition due to the exponential formulation used for the combustion and gas absorption submodels. These submodels participate in the simulation through the source terms of the discretized gas phase governing equations and in particular the energy equation, and they may lead to a high level of stiffness of the solution as described by Roache [19]. To remedy partly this particular difficulty, the source term in the energy equation, which uses the temperature as the dependent variable, is *lagged* by one time step. The formulation employed, based on extensive numerical testing, requires for accuracy and stability that the restrictions imposed by the Courant number [19, 20] be satisfied.

4. EPOXY PROPERTIES

Epoxy (EP) resin is a generic term which is applied to a wide range of materials. These materials contain an epoxy (epoxide) chemical group consisting of an oxygen atom bonded with two carbon atoms. Diglycidyl ether of bisphenol A (DGEBA) resins have the chemical formula $C_{21}O_4H_{34}$ with a molecular weight of 350, and they account for most commercial production of epoxy resins [21].

The parameters required to analyse numerically the ignition delay are given in *table II*, along with their sources of reference.

The largest product of volatiles from the pyrolysis of DGEBA resin at high-boiling under vacuum is phenol; cresols and several substituted mono- and di-nuclear phenols, such as C_2H_5phenols, isopropylphenol, isopropenylphenol and bisphenol A, are also produced in small quantities [21]. To estimate the radiation absorption coefficient and combustion kinetics, the volatiles are assumed to be made up of phenol (C_6H_6O) only, due to its dominating concentration.

On a complete combustion basis, volatiles react with oxygen at a stoichiometric ratio of 1:2.38 on a molal basis:

$$C_6H_6O + 7\,O_2 \longrightarrow 6\,CO_2 + 3\,H_2O$$

TABLE II
Physical, kinetic and radiative properties of epoxy (EP).

Property	Value	Unit	Reference
Molecular weight of volatiles	94	$g \cdot mol^{-1}$	
Density of virgin EP	1 200	$kg \cdot m^{-3}$	Pal et al. [26]
Thermal conductivity of EP	0.20	$W \cdot m^{-1} \cdot K^{-1}$	Pal et al. [26]
Specific heat of EP	1.8	$kJ \cdot kg^{-1} \cdot K^{-1}$	Lee and Neville [21]
Heat of combustion of volatiles	29.83	$MJ \cdot kg^{-1}$	Lewin et al. [22]
Frequency factor of combustion	10^9	$m^3 \cdot kg^{-1} \cdot s^{-1}$	Krishnamurty et al. [28]
Activation energy of combustion	85	$KJ \cdot mol^{-1}$	Krishnamurty et al. [28]
Heat of gasification	2.23	$MJ \cdot kg^{-1}$	Lewin et al. [22]
Frequency factor of gasification	$3 \cdot 10^{10}$	$m \cdot s^{-1}$	Hong and Wang [29]
Activation energy of gasification	134	$kJ \cdot mol^{-1}$	Hong and Wang [29]
Stoichiometric ratio	2.38		
Refractive index of EP	1.55–1.61		Harper [30]
Surface reflectivity of EP	0.05		*
Surface emissivity of EP	0.79		Lubin [31]
Rad. absorp. coef. of EP	$3.4 \cdot 10^4$	m^{-1}	Ohlemiller et al. [2]
Rad. absorp. coef. of volatiles	4	$N^{-1} \cdot m$	*

* present work estimate.

The reaction is exothermic and the heat of combustion is 29.83 MJ per kilogram of epoxy [22].

The absorption spectrum of phenol is reported by Pouchert [23], and it is 90 % transparent to an optical beam and 80 % to a CO_2 laser beam. The transparency of phenol to an optical beam has approximately the same value of that for PMMA to an optical beam. Thus, the absorption radiation at the optical wavelength is estimated to be of the order of magnitude 2 $N^{-1} \cdot m$ by Brosmer and Tien [24], and Amos and Fernandez-Pello [25]. Therefore, the absorption coefficient of phenol for a CO_2 laser beam is estimated to be 4 $N^{-1} \cdot m$ by applying Beer's law to both optical and CO_2 laser wavelengths.

Infrared (IR) band ranges for DGEBA resin are presented by Lee and Neville [21], and they indicate that the transmission of radiation beams is strongly related to the wavelength. In the visible wavelength, the hydroxyl, methyl, and methylene groups will absorb most of the radiation, while the epoxy group is effectively close to the CO_2 laser beam wavelength (10.6 μm). The relation between transmittance and wavelength is different for different epoxies, as illustrated by Lee and Neville [21], who report the IR spectra for 63 different kinds of uncured epoxy resins. Furthermore, it is noted that the intensity of transmittance can be changed by the presence of diluents, additives, curing agents, or impurities, and the absorption bonds shift in the presence of elevated temperatures, also shown by Lee and Neville [21].

The accepted value of the refractive index for DGEBA is 1.5689 [21], and the reflectivity from a surface of epoxy by using the Fresnel relation for dielectric materials is determined to be 0.049. Reliability of thermal conductivity measurements is closely related to the removal of the entrapped air from the specimen. However, in general, epoxy resins have thermal conductivity values around 0.2 $W \cdot m^{-1} \cdot K^{-1}$ which is in the range of other rigid plastics [26].

5. NUMERICAL SIMULATION

Here only a few typical tests for the validation of the model are reported; a complete set of tests designed to assess and evaluate the numerical and phenomenological formulation of the model is reported in Esfahani [9]. To determine the sensitivity of the solutions to the grid size, the ignition delay for the laser flux of 0.21 $MW \cdot m^2$ is used to determine the sensitivity to different grid sizes. The ignition delay converges, by refining the grid, to a value of 1.025 s. For a reduction of 33 % of the grid size corresponding to a decrease from 5.55 mm to 4.20 mm, the ignition delay varies by 17 %, while the variation

is only 1 % when the grid is decreased by 33 % from 1.90 mm to 1.40 mm. It can be noticed, as expected, that solution convergence increases with decreasing grid size.

The temperature profiles along the centreline of the plume predicted for the time of 1 s with five different grid sizes nearly coincide away from the surface. However grid sizes greater than 2.80 mm yield poor resolution in the vicinity of the surface. Therefore, a power grid distribution was employed to increase the resolution near the surface while still placing the top boundary condition at an appropriate distance away from the high temperature region at moderate cost. Typical time step sizes in the vicinity of ignition are of the order of 5 μs.

The two-dimensional solid region, mimicking epoxy, is based on *real* dimensions of 6.35 mm for the width and of 2.5 mm for the thickness, and is located at the lower end of the computational domain which is 6.35 mm wide and 15 mm high. The buoyancy-driven flow of air, volatiles and combustion products occurs right above the epoxy, and the computational region was chosen large enough to capture the main features of the ignition process in what concerns time development of temperature, fuel fraction and velocity. The ignition is initiated by incident radiation that heats up a 4.5 mm patch at the central region of the epoxy surface in contact with the ambient. The physical properties are selected in the range of those typical for epoxy and for air/combustion gases at atmospheric conditions.

TABLE III
Comparison of numerical predictions against the experimental results of Ohlemiller and Summerfield [2].

External source flux, ($MW \cdot m^{-2}$)	Exp. (ms)	Num. (ms)	Error (%)
1	196.0047	196.80	0.41
2	69.9476	70.20	0.36
3	38.2830	39.80	3.96
4	24.9620	26.85	7.56

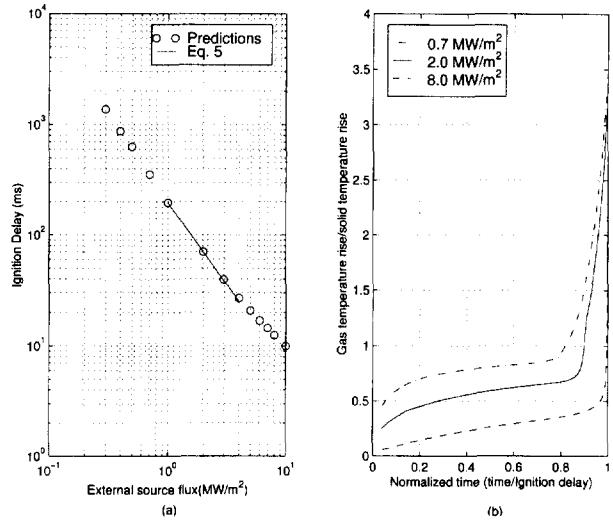

Figure 2. Analyses for epoxy subjected to an incident radiation. **a.** Variation of ignition delay with external source power. **b.** Development of the ratio between the temperature rise rate of the gas phase and the surface temperature rise rate of the solid phase.

6. RESULTS AND DISCUSSION

Predicted ignition delays for external source fluxes in the range of the experiments of Ohlemiller and Summerfield [2] are shown in *table III*. The deviation between predictions and experiments increases with increasing source fluxes, which may be attributed to two causes: the *lag* in the experimental method used, which may have an increasing influence in decreasing ignition delays, and the *uncertainty* in the dynamic values for the properties.

The selected experimental data of Ohlemiller and Summerfield [2] are correlated using least-squares fitting by the following equation:

$$\log t_{ig} = 2.2923 - 1.4865 \log I$$

where t_{ig} (ms) and I ($MW \cdot m^{-2}$) denote ignition delay and laser flux, respectively. The estimated accuracy of the equation is ± 0.7 % for a validity range of 1 to 4 $MW \cdot m^{-2}$.

The numerical predictions and the correlation for the experimental results, equation (5), are depicted in *figure 2a*. The numerical predictions were conducted for a range of laser flux values wider than those for the experiments covered by equation (5) with the objective of showing the versatility of the model. In general, the predictions are in good agreement with the experiments. However this agreement tends to deteriorate, as already mentioned, with increasing values of the laser flux. At higher fluxes, the time to heat the solid phase to a high temperature is very short as compared to the time required for diffusional processes to warm up the gas phase and to reach the required ignition conditions. As shown in *figure 2b*, the values of the ratio between the temperature rise rate of the gas phase and the surface temperature rise rate of the solid phase decrease with increasing heat fluxes prior to ignition, with an asymptotic value of zero. Therefore, at extremely high fluxes, the ignition just requires time to diffuse heat and volatiles in the gaseous phase, while the surface of the solid reaches an *instantaneous* ready-for-ignition state. This argument may yield the conclusion that for extremely high fluxes, ignition will occur at an asymptotic value for the time delay.

The temperature distribution at the threshold of ignition for two different fluxes, 8 $MW \cdot m^{-2}$ and 0.7 $MW \cdot m^{-2}$, is shown in *figure 3*. For the higher laser flux (8 $MW \cdot m^{-2}$), the temperature isotherms are stratified with relation to the surface, and the ignition occurs at the periphery of the irradiated spot, as observed by Ohlemiller and Summerfield [2] employing high speed movies. The dispersion of heat in the gas phase is of the order of $\sqrt{\alpha t}$, i.e. 0.5 mm at the threshold of ignition with the power source of 8 $MW \cdot m^{-2}$. For the lower flux (0.7 $MW \cdot m^{-2}$), the ignition, rather than occurring at one single spot, occurs in a layer parallel to the surface, while the spreading of the thermal plume is very low, which can be explained on the basis of the velocity fields.

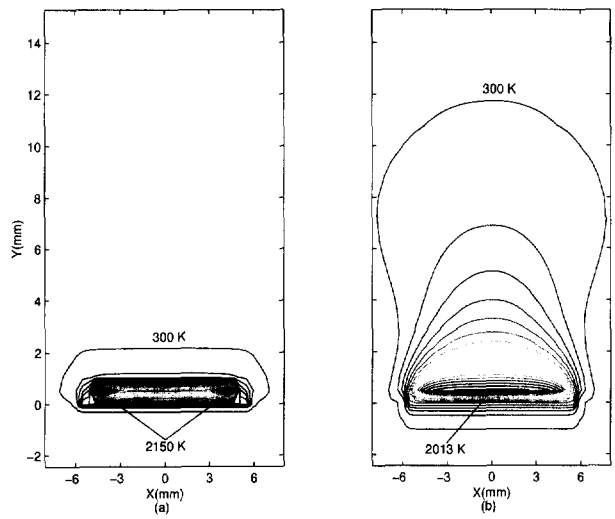

Figure 3. Analyses for epoxy subjected to incident radiation. Temperature contour distribution at the threshold of ignition for two different external power sources: **a.** 8 $MW \cdot m^{-2}$, and **b.** 0.7 $MW \cdot m^{-2}$, (isotherms are plotted at 100 K intervals).

The velocity field at the threshold of ignition for the two different fluxes, 8 $MW \cdot m^{-2}$ and 0.7 $MW \cdot m^{-2}$, is shown in the *figure 4*. A circulation occurs at the lower flux (0.7 $MW \cdot m^{-2}$), *figure 4b*, while, at the higher flux (8 $MW \cdot m^{-2}$), the flow field behaves as a free jet from the surface, *figure 4a*. This can be explained on the view that for higher fluxes the momentum due to the volatiles production is much higher than that for buoyancy, while the shear forces acting upon the upward flow of the volatiles force the flow to turn to the periphery of the beam. For the lower heat flux (0.7 $MW \cdot m^{-2}$), *figure 4b*, the entrainment of air at the periphery prevents the spreading of the plume, while for the higher heat fluxes (8 $MW \cdot m^{-2}$), *figure 4a*, the flow turns towards the periphery of the hot spot causing heat and volatiles to be advected away from the hot spot. This explains why the location of the highest temperature is strongly related to the velocity field,

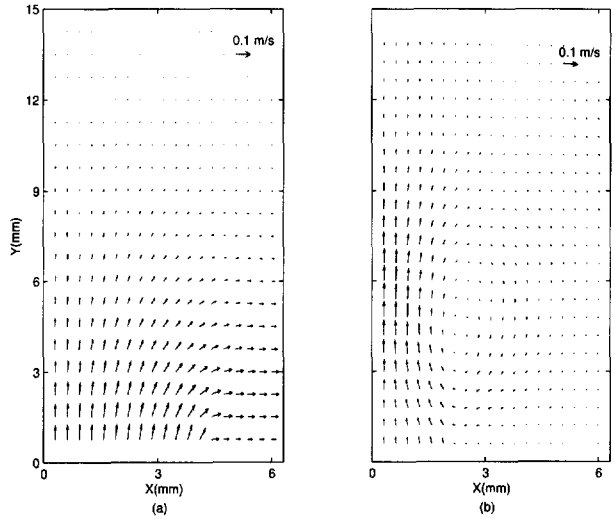

Figure 4. Analyses for epoxy subjected to incident radiation. Velocity field at the threshold of ignition for two different external power sources: **a.** 8 $MW \cdot m^{-2}$, and **b.** 0.7 $MW \cdot m^{-2}$.

which is itself related to the power of the external heat flux.

The velocity field for high fluxes closely resembles the velocity field for the low fluxes in microgravity [7]. This is an interesting, but not unexpected, result, as buoyancy plays no role for high flux ignition while low flux ignition in microgravity is altogether absent. Extension of this similarity, however, requires considerable caution, since: i) thermal degradation will be different for different fluxes, and ii) the attenuation of radiation by volatiles may play an important role, as reported by Esfahani and Sousa [27].

The results for epoxy indicate that the attenuation of radiation by the gas is practically negligible. This is readily justified by noting that the diffusion length of volatiles in the gas phase and the radiation absorption coefficient of volatiles are approximately 1 mm and 4 $N^{-1} \cdot m$, respectively. Using Beer's law to calculate attenuation yields a value of less than 0.4 %. The attenuation coefficient of cresol, the largest component of the volatiles after phenol, is about 50 % higher than that of phenol. Its effect upon attenuation, however, can be neglected. For cresol as the only component of the volatiles, the value of the attenuation would be less than 0.6 %. This low influence can be attributed to its relatively small diffusion length and concentration. Thus, selecting phenol as the only component of the volatiles does not affect the results, because of the magnitude of the attenuation coefficient for the range of values considered for the external power source.

The assumption of phenol-only volatiles may affect the results through the combustion kinetics. However data are not readily available. Ignition delay has high sensitivity to the activation energy of combustion.

For instance, with an external radiation source of 2 $MW \cdot m^{-2}$, predictions indicate that the ignition delay decreases by 5 % when the activation energy increased 10 %.

7. CONCLUDING REMARKS

The numerical model yields predictions which compare well with the published experimental data. Predictions are well within the uncertainties related to the experimental methodologies and the input thermal and chemical properties required by the simulation. These properties are obtained from sources in the literature, and they may take different values for similar products, but produced by different manufacturers. Also, the dynamic values for combustion reaction, degradation, and radiation are not readily available.

The predictions yield the following findings and observations:

- the location of the highest temperature just prior to the threshold of ignition is strongly related to the velocity field, which is itself related to the power of the external heat flux, and the thermal degradation process rate;

- the convective flow above the heated surface is characterized by a strong recirculation for the lower flux (0.7 $MW \cdot m^{-2}$), while, at the higher flux (8 $MW \cdot m^{-2}$), the flow behaves as a free jet from the surface, resembling the flows prevailing in microgravity tests;

- the values of the ratio between the temperature rise rate of the gas phase and the surface temperature rise rate of the solid phase are decreasing for increasing heat fluxes prior to ignition, with an asymptotic value tending to zero;

- at very high fluxes, the ignition delay is controlled by the time required to diffuse heat and volatiles in the gaseous phase, as the surface of the solid reaches the ignition potential at negligible time. This argument may yield the conclusion that the ignition delay may tend to an asymptotic value at extremely high fluxes.

This novel modelling methodology demonstrated the importance of the flow field upon the ignition process, and in particular upon the thermal stratification. A major advantage of the methodology is its potential use in safety and prevention analysis to identify and track the eventual toxic volatiles emanating from materials in enclosed spaces.

Acknowledgment

This work was supported by Natural Sciences and Engineering Research Council of Canada grant OGP0001398 (ACMS), and one of the authors (JAE) also acknowledges the support received from Ferdowsi University, Mashhad, Iran.

RÉFÉRENCES

[1] Rose N., Le Bras M., Bourbigot S., Delobel R., Thermal oxidative degradation of epoxy resins: evaluation of their heat resistance using invariant kinetic parameters, Polymer Degradation and Stability 45 (1994) 387–397.

[2] Ohlemiller T.J., Summerfield M., Radiative ignition of polymeric materials in oxygen/nitrogen mixtures, in: 13th International Symp. on Combustion, The Combustion Institute, Pittsburgh, USA (1971) 1086–1094.

[3] Nelson M.I., Brindley J., McIntosh A.C., The effect of heat sink additives on the ignition and heat release properties of thermally thin thermoplastics, Fire Safety J. 28 (1997) 67–94.

[4] Di Blasi C., Crescitelli S., Russo G., Cinque G., Numerical model of ignition process of polymeric materials including gas-phase absorption of radiation, Combust. Flame 83 (1991) 333–334.

[5] Chandrasekaran V., Brescianini C.P., Yeoh G.H., Grubits S.J., Yuen R., A numerical model for the prediction of pilot ignition of PMMA, Adv. Fluid Mech. 9 (1996) 156–166.

[6] Quintiere J., Some observation on building corridor fires, in: 15th (Int) Symp on Combustion, The Combustion Institute, Pittsburgh, USA (1975) pp. 163–174.

[7] Ramachandra P.A., Altenkirch R.A., Bhattacharjee S., Tang L., Sacksteder K., Wolverton M.K., The behavior of flames spreading over thin solids in microgravity, Combust. Flame 100 (1995) 71–84.

[8] Kashiwagi T., Polymer combustion and flammability-role of the condensed phase, in: 25th International Symposium on Combustion, The Combustion Institute, Pittsburgh, USA, (1994) pp. 1423–1437.

[9] Esfahani J.A., Numerical studies of the ignition process of charring and non-charring solid materials, PhD thesis, Department of Mechanical Engineering, University of New Brunswick, Canada, 1998.

[10] Kashiwagi T., Effects of sample orientation on radiative ignition, Combust. Flame 44 (1982) 223–245.

[11] Hawkins W.L., Polymer degradation and stabilization, Springer-Verlag, Berlin, Heidelberg, 1984.

[12] Esfahani J.A., Sousa A.C.M., Lopes A.M.G., Numerical modeling of ignition by radiation for a cellulosic material, in: Wrobel, L.C. et al. (Eds), Computational Modelling of Free and Moving Boundary Problems. III. Computational Mechanics Publications, Southampton, UK, 1995, pp. 327–334.

[13] Ohlemiller T.J., Modelling of smoldering combustion propagation, Prog. Energy Combust. Sci. 11 (1985) 277–310.

[14] Sparrow E.M., Cess R.D., Radiation Heat Transfer, Brooks/Cole Publishing Co, California, USA, 1970.

[15] Patankar S.V., Numerical Heat Transfer and Fluid flow, Hemisphere Pub. Co, Washington DC, USA, 1980.

[16] Van Doormaal J.P., Raithby G.D., Enhancements of the SIMPLE method for predicting incompressible fluid flows, Numer. Heat Tr. 7 (1984) 147–163.

[17] Braaten M.E., Shyy W., Study of pressure correction methods with multigrid for viscous flow calculation in non orthogonal curvilinear coordinates, Numer. Heat Tr. 11 (1987) 417–442.

[18] Lopes A.M.G., Sousa A.C.M., Viegas D.X., Numerical simulation of turbulent flow and fire propagation in complex topography, Numer. Heat Tr. A 27 (1995) pp. 229–253.

[19] Roache P.J., Computational Fluid Dynamics, Hermosa Publishers, Albuquerque, New Mexico, USA, 1972.

[20] Satoh K., Lloyd J.R., Yang K.T., Kanury A.M., A numerical finite-difference study of the oscillatory behavior of vertically vented compartments, in: Shih T.M. (Ed.), Numerical Properties and Methodologies in Heat Transfer, Hemisphere Publishing Corporation, USA (1983) 517–528.

[21] Lee H., Neville K., Handbook of epoxy resins, McGraw-Hill, 1967.

[22] Lewin M., Atlas S.M., Pearce E.M., Flame-retardant Polymeric Materials, Plenum Press, New York, 1982.

[23] Pouchert C.J., The Aldrich Library of Infrared Spectra, Milwaukee Wisconsin, Aldrich Chemical Co, 1975.

[24] Brosmer M.A., Tien C.L., Radiative energy blockage in large pool fires, Combust. Sci. Technol. 51 (1987) 21–37.

[25] Amos B., Fernandez-Pello A.C., Model of the ignition and flame development on a vaporizing combustible surface in a stagnation point flow: ignition by vapor fuel radiation absorption, Combust. Sci. Technol. 62 (1988) 331–343.

[26] Pal G., Macskasy H., Plastics: Their Behaviour in Fires, Elsevier, New York, USA, 1991.

[27] Esfahani J.A., Sousa A.C.M., Effect of attenuation of radiation on the ignition process in quiescent air, in: 3rd International Thermal Energy Congress, Kitakyushu, Japan, 1997, pp. 169–174.

[28] Krishnamurthy L., Williams F.A., Laminar combustion of polymethylmethacrylate in O_2/N_2 mixtures, in: 14th International Symp on Combustion, The Combustion Institute, Pittsburgh, USA, 1973, pp. 1151–1164.

[29] Hong S.G., Wang T.C., Effect of copper oxides on the thermal oxidative degradation of the epoxy resin, J. Appl. Polym. Sci. 52 (1994) 1339–1351.

[30] Harper C.A., Handbook of Plastics and Elastomers, McGraw-Hill, USA, 1992.

[31] Lubin G., Handbook of fiberglass and advanced plastics composites, Reinhold Book Co, New York, USA, 1969.